Physica E 135 (2022) 114950

Contents lists available at ScienceDirect

Physica E: Low-dimensional Systems and Nanostructures

journal homepage: www.elsevier.com/locate/physe

A density functional theory study on favipiravir drug interaction with BN-doped C60 heterofullerene

İskender Muz [a,*], Fahrettin Göktaş [b], Mustafa Kurban [c,**]

[a] Department of Mathematics and Science Education, Nevşehir Hacı Bektaş Veli University, 50300, Nevşehir, Turkey
[b] Department of Energy System Engineering, Ankara Yıldırım Beyazıt University, 06170, Ankara, Turkey
[c] Department of Electrical and Electronics Engineering, Kırşehir Ahi Evran University, 40100, Kırşehir, Turkey

ARTICLE INFO

Keywords:
$C_{30}B_{15}N_{15}$ heterofullerene
Favipiravir
Adsorption
DFT
Drug delivery

ABSTRACT

We have performed to study the possibility of a stable interaction between favipiravir drug molecule and BN-doped C_{60} (CBN) heterofullerene. The structural, electronic, reactivity and optical properties for the mentioned interactions are examined in detail. Adsorption energies between favipiravir drug and CBN heterofullerene are calculated in the range of −3.41 and −23.95 kcal/mol. The adsorption energy of configuration **A** is −23.95 kcal/mol means that B–O bonding in configuration **A** is stronger than that of B–N and C–O in other configurations. The results mean that the O atom of favipiravir interacts strongly with B atom of the heterofullerene. The smallest value of the E_g (0.4 eV) means that charge transfer can easily occur between occupied and unoccupied orbitals of the favipiravir and CBN heterofullerene. The charge transfer from adsorbed the favipiravir to CBN heterofullerene was confirmed by the WBI and FBO analyses. From the absorption peaks obtained UV–visible (UV–vis) spectra indicate that all configurations can absorb in the visible light region. Finally, these results may guide drug delivery systems.

1. Introduction

Today's viruses have become a global health problem and are among the main causes of mortality in the world. Therefore, there is now an urgent need for novel perspectives to virus treatments more specific and effective [1].

Favipiravir also known as avigan or T-705 is an antiviral drug against viruses [2] and has the potential to treat many viral infections including Ebola [3–5] and Sars-Cov-2 [6,7]. It has been subjected to numerous studies related to the drug development industry up to date [8]. Especially, favipiravir is also one of many approved drugs being tested as a possible treatment for Covid-19, and so it is nowadays a hot topic.

Traditional drugs like oral and injection medicines are quickly and extensively spread in the body, affecting adversely many systems and causing the manifestation of the side and toxic effects [9]. In addition, it can be sometimes necessary to use higher doses of a drug in order to achieve the desired effect [10]. Nanotechnology plays a vital role in drug the delivery [11] and has always made it easy to control the place and time as well as the speed of drug release in the body [12,13]. In recent years, C_{60} fullerenes as carrier material have been utilized for delivery of many drugs to specific diseased cells [14–23]. Similarly, fullerene derivatives also have been widely used in many applications as nanocarriers [24] due to their various advantages such as decreasing the side effects, increasing the efficacy of the drug and highly symmetrical spherical nanoparticles. It has concluded that the C_{60} fullerene may lead to $\pi-\pi$ stacking interaction with some drug molecules [25] while doping the C_{60} through impurity atoms is among the best methods to change the weak $\pi-\pi$ stacking interactions to the strong chemical bonds [26]. With impurity atom substitutions, it is also possible to change the charge distribution properties of fullerene, which leads to a significant increment of the adsorption properties of them and makes them possible candidates as sensors by causing changes in the energy gap [27,28]. In addition, fullerene and its derivatives also have been widely used in many applications as nanocarriers due to their various advantages such as decreasing the side effects and increasing the efficacy of the drug as well as high thermal stability, highly symmetrical spherical nanoparticle, and high solubility in biological fluids [29,30]. The BN-doped C_{60} (CBN) heterofullerene is the most commonly used among fullerene derivatives and firstly reported by Erkoç [31], who proposed that it is a good candidate for optical applications due to its

* Corresponding author.
** Corresponding author.
E-mail addresses: iskendermuz@yahoo.com (İ. Muz), mkurbanphys@gmail.com (M. Kurban).

https://doi.org/10.1016/j.physe.2021.114950
Received 7 January 2021; Received in revised form 12 August 2021; Accepted 27 August 2021
Available online 1 September 2021

optimum bandgap and its unique properties [32–34]. In spite of the wide applications for C_{60} fullerenes the theoretical studies of the interaction with different drugs are actually quite a few, there has been only one limited study of the interaction of drug molecules with CBN heterofullerene [35]. In that study, it is reported that CBN heterofullerene is utilized as a carrier to deliver the isoniazid molecules [35]. To the best of our knowledge, there is no study of the interaction of favipiravir drug molecule with CBN heterofullerene. Besides, it is important to know that long-term clinical trials and experimental researches are needed to assess the efficacy of prepared drug samples, but to obtain beforehand enough information; computational-based researches may provide a fast and safe way in order to find the most promising samples for drug development.

The main aim of this study was to employ density functional theory (DFT) in association with the B3LYP functional to clarify the possible interaction mechanism of CBN heterofullerene with favipiravir drug molecule and to understand the potential use of CBN heterofullerene as a drug delivery tool. Within this framework, it is aimed to determine whether CBN heterofullerene adsorb favipiravir molecule as a drug carrier candidate.

2. Computational details

Using DFT calculations based on the reliable B3LYP functional with basis set 6-31G (d,p) [36] and an empirical dispersion term of Grimme's three-parameter [37], we have performed to study the possibility of a stable interaction between favipiravir drug molecule and CBN heterofullerene. To model the possible interactions, the favipiravir drug molecule and CBN heterofullerene were optimized and then the position of the drug around heterofullerene based on the structure the lowest energies were tested. Optimized structures and their vibrational frequencies were carried out using Gaussian 09 [38].

The adsorption energy (E_{ad}) between favipiravir drug molecule and CBN heterofullerene is calculated using the following expression:

$$E_{ad} = E(CBN + Drug) - E(CBN) - E(Drug) + E(BSSE)(1)$$

where $E(CBN + Drug)$ is the total energies of the adsorbed favipiravir on CBN heterofullerene. $E(CBN)$ and $E(Drug)$ are the total energies of CBN heterofullerene and favipiravir, respectively. $E(BSSE)$ is known as the "basis set superposition error", which is calculated by the counterpoise method to achieve highly accurate adsorption energy functional prediction [39].

The B3LYP functional gives systematically underestimate HOMO/LUMO energies. Moreover, an efficient way to transmit accurate HOMO/LUMO energies is to use a range-separated functional, such as those used in the following studies to obtain accurate energies [40,41]. We should also mention that the structures studied here are very large with high degrees of freedom which make it very difficult to use larger basis sets. Therefore, 6-31G (d, p) basis set which contains a reasonable number of basis set functions was used for the calculations.

The vertical ionization potential (VIP) and vertical electron affinity (VEA) are calculated using the following expressions: [$VIP = E^{cation} - E^{neutral}$] and [$VEA = E^{neutral} - E^{anion}$]. In these expressions, the VIP is the energy difference between the ground state of the cation (E^{cation}) and the ground state of the neutral ($E^{neutral}$) at the geometry of the neutral. VEA is defined as the energy difference between the ground state of the neutral and the ground state of the anion (E^{anion}) at the geometry of the neutral. Besides, the chemical hardness (η), electrophilicity index (ω) and the maximum amount of electronic charge index (ΔN_{tot}) are also calculated. It is also worth to note that a hard molecule corresponds to a large energy gap as a manifestation of the principle of maximum hardness [42]. ω and ΔN_{tot} parameters are also defined as a measure of the ability of a specification to accept electron.

For favipiravir drug molecule adsorbed on the CBN heterofullerene, the Wiberg bond index (WBI) and Fuzzy bond orders (FBO) are performed using the Multiwfn program [43].

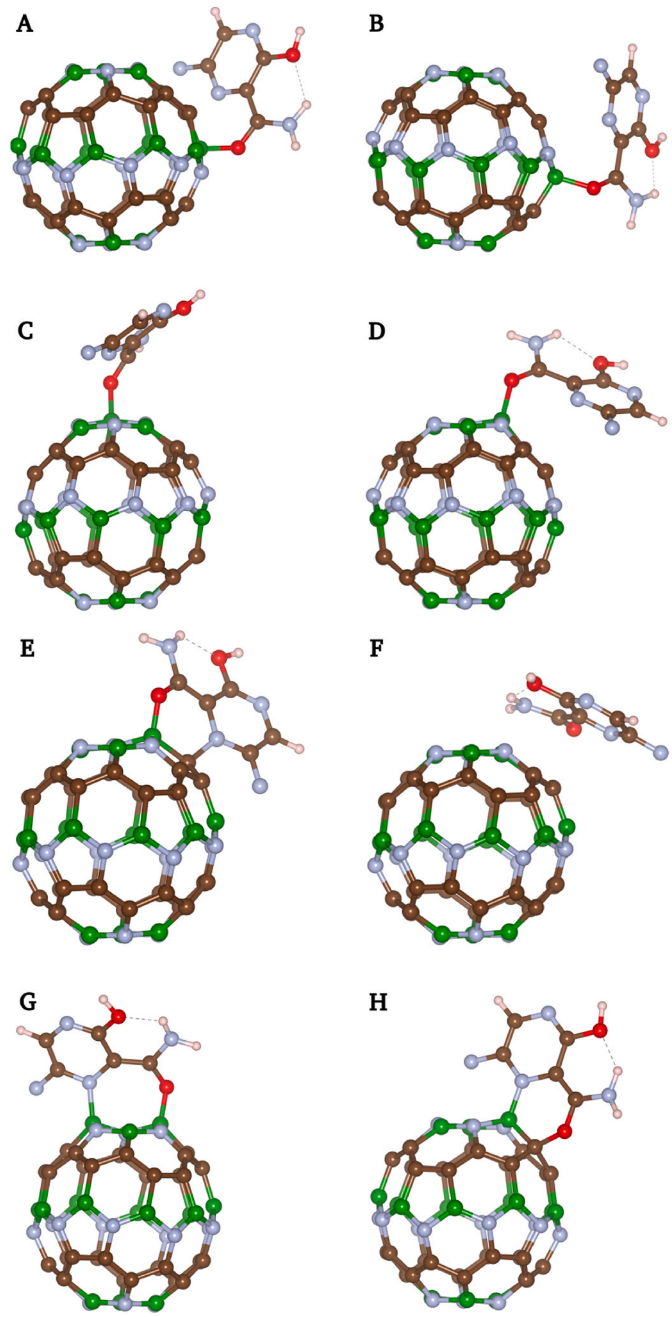

Fig. 1. (Colour online) The optimized configurations of favipiravir adsorbed on CBN heterofullerene computed at B3LYP/6-31G(d) level of theory (Green (B), Brown (C), Blue (N), Purple (H), Red (O)).

3. Results and discussions

In DFT calculations, obtaining a good initial guess during energy optimization is a key factor to find out proper geometry with the lowest energy conformation, thus, it is important to consider all possible configurations when different systems interact with each other. Moreover, there is no negative frequency that implies the transition state at a saddle-point. In this context, possible interactions between CBN heterofullerene and favipiravir drug molecule were performed and among obtained structures, eight different configurations were evaluated and sorted according to relative energies (ΔE) in this study, as depicted in Fig. 1. The relative and adsorption energies of theoretically predicted

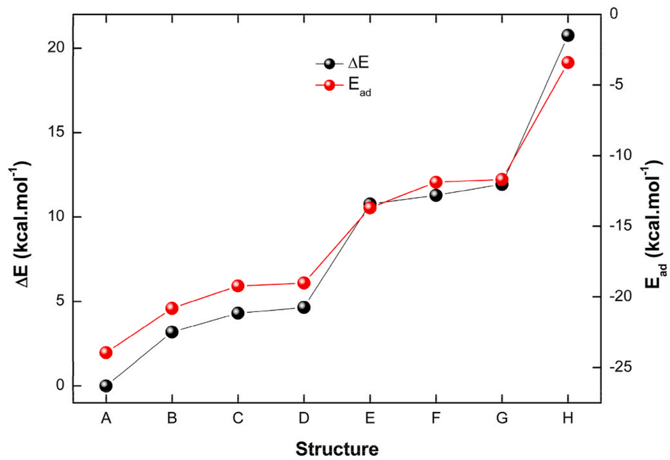

Fig. 2. (Colour online) Relative energy (ΔE) and adsorption energy (E_{ad}) for the optimized configurations of favipiravir adsorbed on CBN heterofullerene.

geometries are shown in Fig. 2. Depending on the location of the favipiravir on CBN heterofullerene, large changes of the ΔE were predicted at the B3LYP level. In this study, the ΔE of configuration **A** is found to be the configuration with lowest energy where a single O atom from the favipiravir is bounded to B atom of the CBN heterofullerene. On the other hand, the ΔE of configuration **B** is predicted as 3.19 kcal/mol which is much higher than the most stable configuration. The ΔE of configurations **C, D, E, F** and **G** are found as 4.31, 4.65, 10.77, 11.28 and 11.93 kcal/mol, respectively. The ΔE is found as 20.76 kcal/mol which is the biggest value among other configurations, when N and O atoms from the favipiravir are bounded to C and B atoms of the CBN heterofullerene (configuration **H**). The considerable fluctuations in the ΔE are due to the interactions between N and O atoms of the favipiravir and the B and C atoms of the CBN heterofullerene in the different positions. When it comes to the adsorption energies (E_{ad}), which are calculated in the range of −3.41 and −23.95 kcal/mol, O atoms from the favipiravir interacts strongly with B atoms of the CBN heterofullerene. The negative E_{ad} reveals that favipiravir adsorption onto the CBN heterofullerene surface was an exothermic process and energetically favorable. The interaction between O atoms of the favipiravir and B atom of the CBN

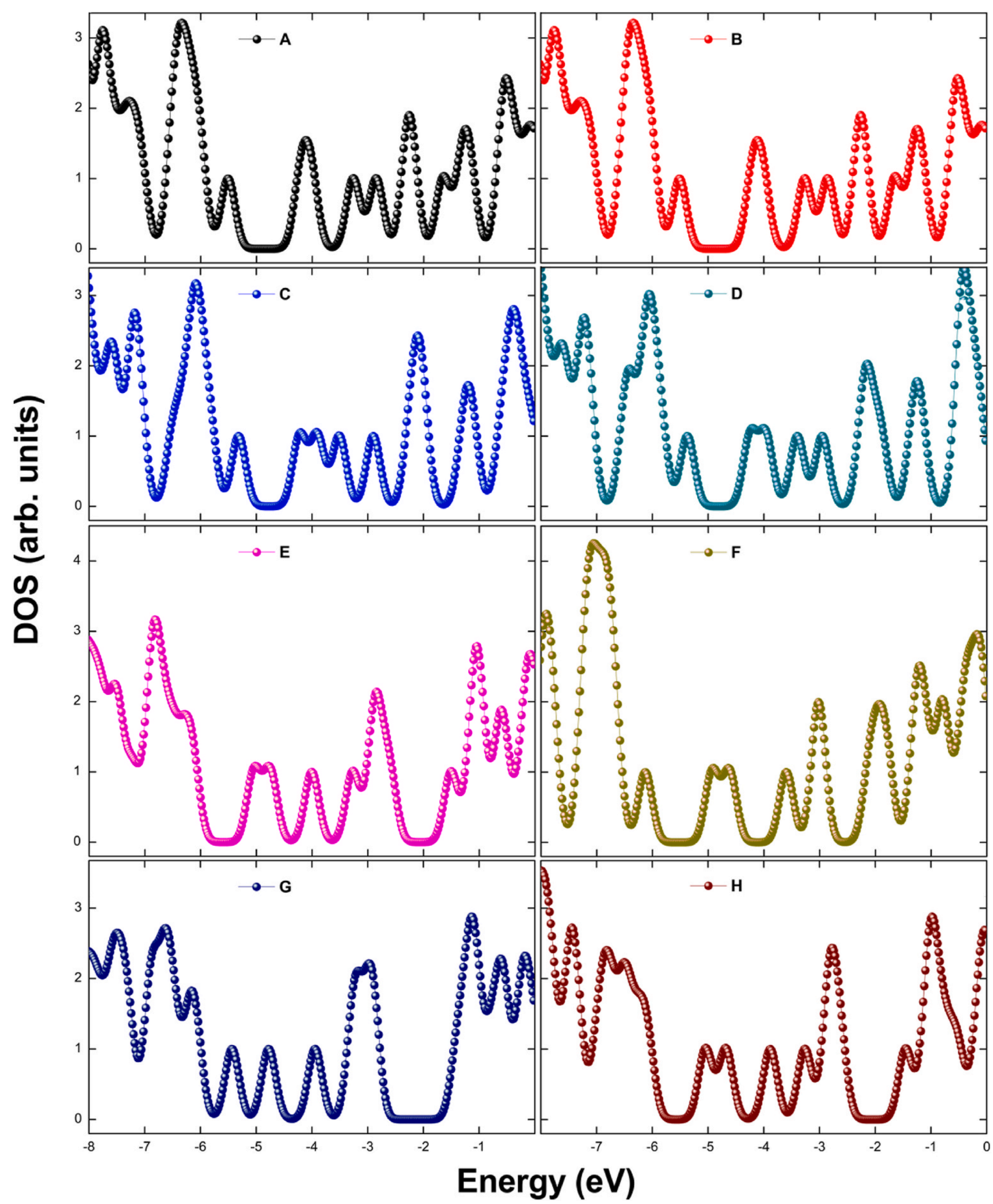

Fig. 3. (Colour online) Density of states (DOS) for the optimized configurations of favipiravir adsorbed on CBN heterofullerene.

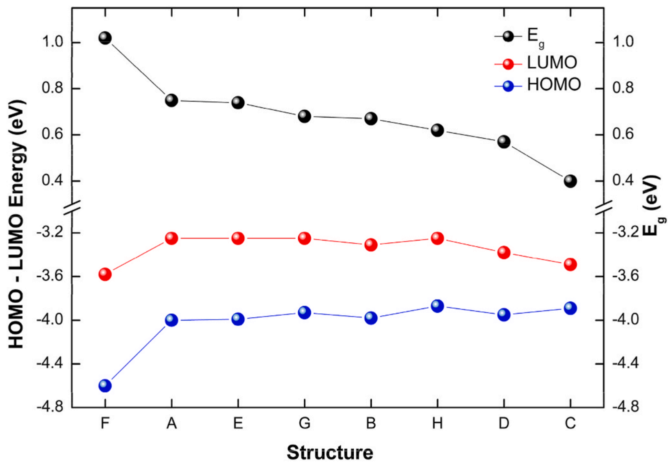

Fig. 4. (Colour online) HOMO, LUMO energy and HOMO-LUMO energy gap (E_g) for the optimized configurations of favipiravir adsorbed on CBN heterofullerene.

heterofullerene in the different positions have an important influence on the E_{ad}. In addition, binding of N atom from the favipiravir to CBN heterofullerene significantly decreases the E_{ad}. We note that configuration **A** with most negative interaction energy −23.95 kcal/mol is more favorable than the other configurations **B** (−20.81 kcal/mol)**, C** (−19.22 kcal/mol)**, D** (−19.01 kcal/mol)**, E** (−13.69 kcal/mol)**, F** (−11.88 kcal/mol)**, G** (−11.69 kcal/mol) and **H** (−3.41 kcal/mol) which means that CBN heterofullerene can be used in drug delivery systems.

The charge transfer between the HOMO and LUMO energy levels is significant physical property for interacting systems [44]. Therefore, the HOMO/LUMO energy levels from density of states (DOS) analysis constructed by GaussSum [45] (see Fig. 3) and the energy gap (E_g) from the energy difference between the HOMO and LUMO for all configurations are carried out to get an insight about the kinetic stability and chemical reactivity of the studied configurations, shown in Fig. 4. The HOMO and LUMO values are calculated as about −3.89 and −3.49 eV, respectively, and corresponding the E_g is predicted as 0.4 eV which is the smallest value for configuration **C**. On the other hand, the HOMO and LUMO energy levels for configuration **F** are found as −4.60 and −3.58 eV, respectively. The E_g corresponding to the HOMO and LUMO is 1.02 eV, which is greatest value than the other configurations **A, B, D, E, G** and **H** which change in the range of 0.57–0.75 eV. Overall, the smallest value of the E_g for configuration **C** means that charge transfer can easily occur between HOMO and LUMO energy levels thus gives rise to a change in the biological activity of the favipiravir and CBN heterofullerene configuration. That is, the change the position of the favipiravir on the CBN heterofullerene configuration give rise to an increase in the energy of the HOMO (−3.89 eV) and a decrease in the energy of the LUMO (−3.49 eV) of the configuration **C**, which favorably contributes to a decrease in the E_g, which further contributes to the charge-transfer process [46–48]. In addition, the molecular orbital patterns (HOMO and LUMO) of optimized geometries are presented (see Supporting Information; Figs. S1-S2). The HOMO is localized at the adsorbed favipiravir molecule (for A, E, G and H configurations) and the LUMO is localized at the CBN heterofullerene. When it comes to B, C and D configurations, the HOMO is localized at the CBN heterofullerene and the LUMO is localized at the adsorbed favipiravir, whereas there is no localization in the LUMO for the F configuration. Moreover, the molecular orbitals for HOMO and LUMO seem to be almost the same in the interaction of the parallel-positioned favipiravir molecule with fullerene (F configuration). We note that other configurations except F can be explained by the fact that the band gaps are almost identical to each other (see Fig. S1-S2).

The vertical ionization potential (*VIP*), vertical electron affinity (*VEA*), chemical hardness (η), electrophilicity index (ω), and maximum amount of electronic charge index (ΔN_{tot}) for CBN heterofullerene interacting with the favipiravir configurations are performed to determine how the reactivity properties change with different configurations of the favipiravir on CBN heterofullerene (see Table S1). For the examined configurations, the greater *VIP* value of configuration **F** is 5.73 eV, which decreases to 4.78 eV in the configuration **H** (see Fig. 5). This trend of the *VIP* is because of the increase in HOMO energy levels according to the electron-donating ability of the favipiravir towards CBN heterofullerene. It is obvious that configuration **F** is the most stability than that of the others, which means the large energy required to eject electrons from the configuration **F.** This result is also verified with the HOMO and LUMO energy levels (see Fig. 4). Besides, the configurations **A, B, C, D, E** and **G** have very small difference in values of *VIP*, which are 5.05, 5.04, 5.02, 4.99, 4.99 and 4.86 eV, respectively (see Fig. 5). On the other hand, the greater *VEA* value of configuration **F** is 2.42 eV, which decreases to 2.09 eV in the configuration **A** (see Fig. 5). In addition, the *VEA* of other configurations exhibits small difference, i.e., *VEA* = 2.11 and 2.19 eV for configurations **C** and **E.** The lowest value of η belongs to configuration **C** with a value 0.2 eV which means that configuration **C** is energetically more reactive and demonstrates less resistance to charge transfer than other configurations (see Fig. 5). The trend of variations in η is proportional to the change in the E_g as expected (see Fig. 4).

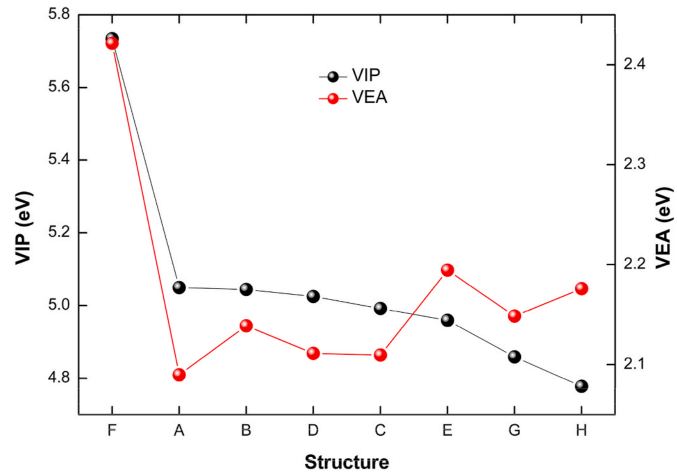

Fig. 5. (Colour online) Vertical ionization potential (VIP) and vertical electron affinity (VEA) for the optimized configurations of favipiravir adsorbed on CBN heterofullerene.

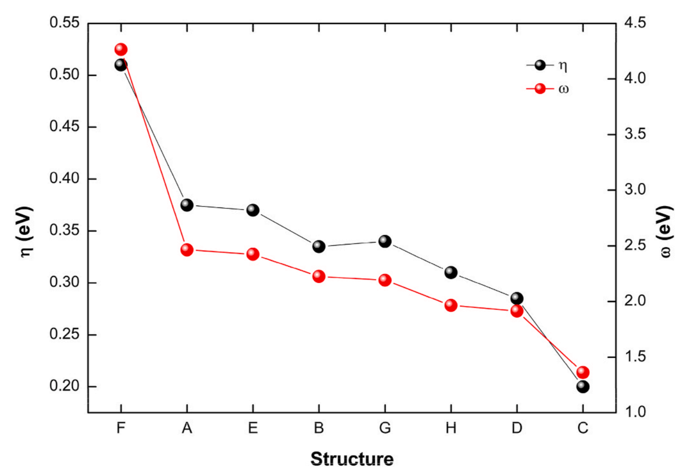

Fig. 6. (Colour online) Chemical hardness (η) and electrophilicity index (ω) for the optimized configurations of favipiravir adsorbed on CBN heterofullerene.

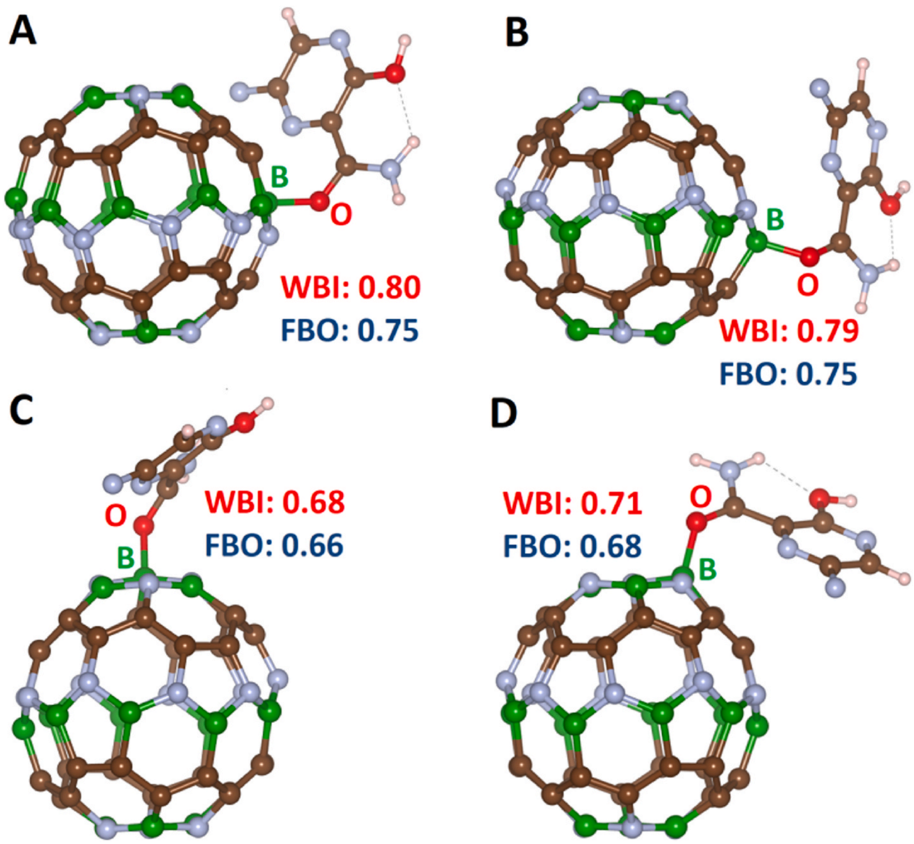

Fig. 7. (Colour online) Wiberg bond index (WBI) and Fuzzy bond order (FBO) for the optimized configurations (**A-D**) of favipiravir adsorbed on CBN heterofullerene.

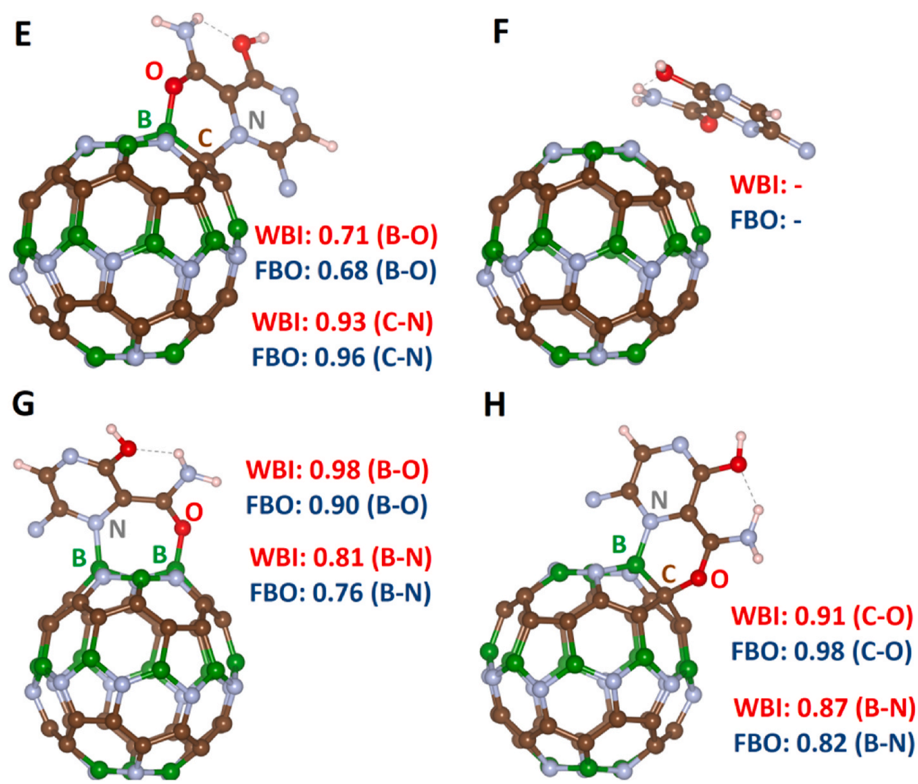

Fig. 8. (Colour online) Wiberg bond index (WBI) and Fuzzy bond order (FBO) for the optimized configurations (**E-H**) of favipiravir adsorbed on CBN heterofullerene.

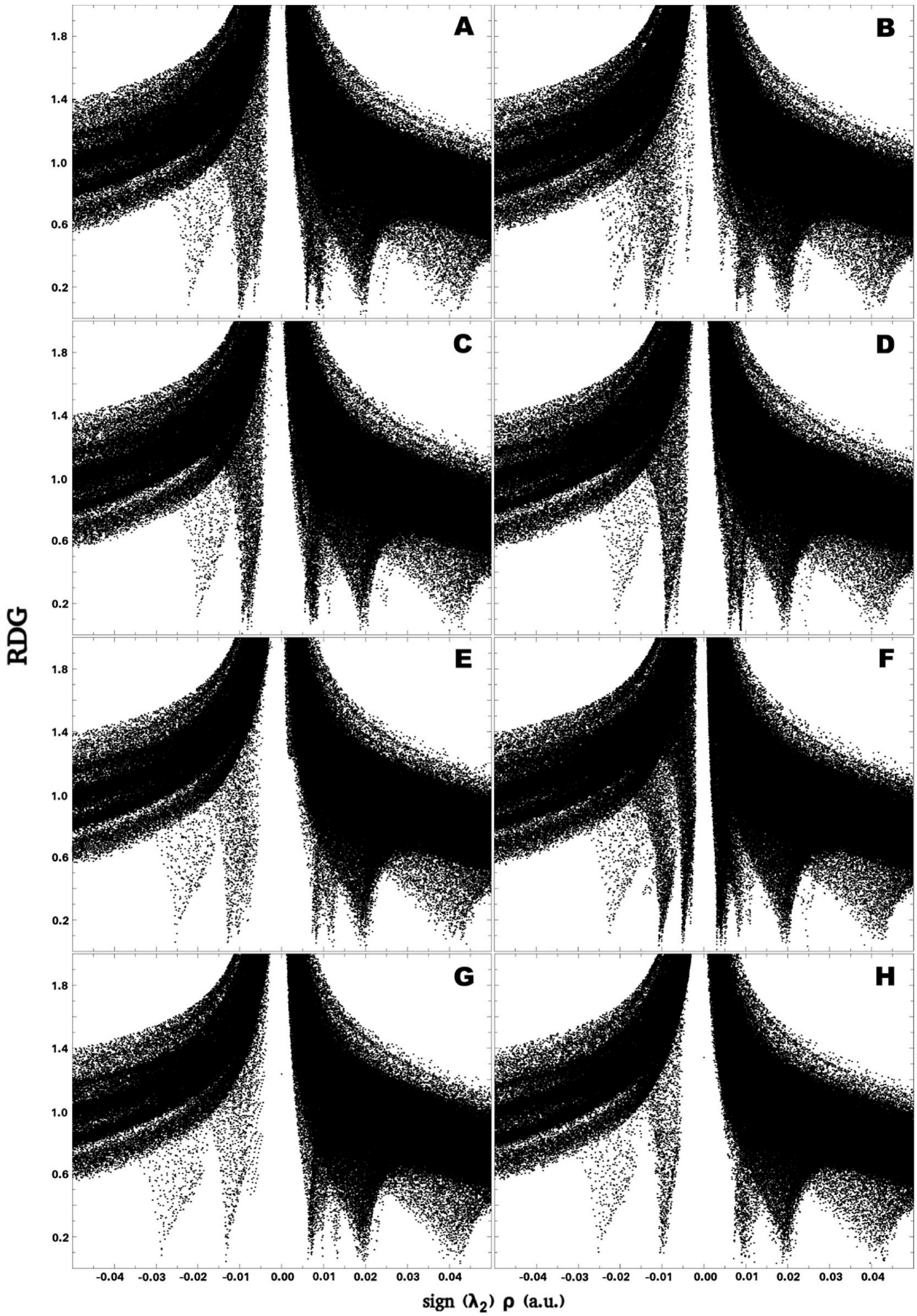

Fig. 9. The reduced density gradient (RDG) scatter plots for the optimized configurations of favipiravir adsorbed on CBN heterofullerene.

To explore the electrophilic features of the examined configurations, electrophilicity indexes (ω) were also investigated. It was found out that configuration **F** has the highest electrophilic character with 4.26 eV while configuration **C** has the smallest value with 1.36 eV (see Fig. 6).

This decrease in η and ω, cause lowering of stability and increase in reactivity of CBN heterofullerene–Favipiravir complex.

Moreover, the maximum amount of electronic charge index (ΔN_{tot}) is researched (see Table S1). The ΔN_{tot} value for configuration **C** are calculated to be 18.45 eV, which is the greatest value, but the ΔN_{tot} of other configuration are found as in the range of 8.01–12.85 eV. Here, it is interesting to note that different configurations of the favipiravir on CBN heterofullerene give rise to an important change in the structural and electronic properties, thus a change in energy stability.

The values of WBI and FBO for eight different interactions between CBN heterofullerene and favipiravir drug molecule were presented in Figs. 7 and 8. The values of WBI and FBO for favipiravir on the CBN

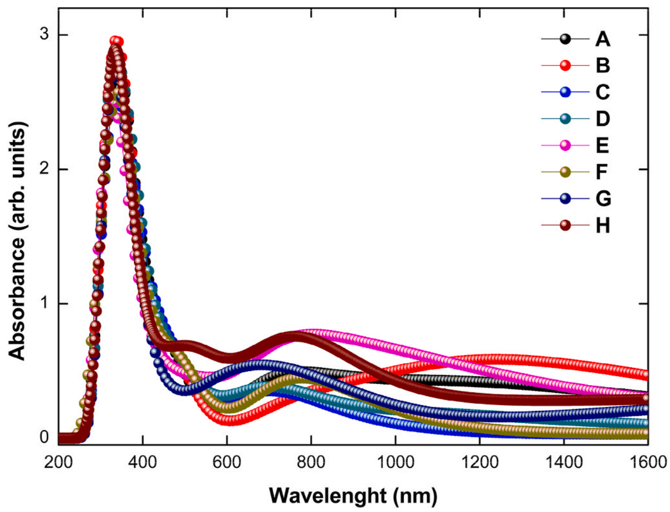

Fig. 10. UV–vis spectra of interacting favipiravir and CBN heterofullerene configurations.

heterofullerene surface for configurations **A** and **B** were calculated about 0.80 and 0.75, respectively. These values for configurations **C** and **D** were found as in the range of 0.68–0.66 and 0.71–0.68, respectively. It is obvious that the B–O interactions of configurations **A** and **B** are stronger than that of **C** and **D.** When N and O atoms from the favipiravir are bounded to C and B atoms of the CBN heterofullerene for configurations **E, G** and **H**, WBO and FBO values vary significantly depending on the binding points of the configurations. For example, the higher values of WBI and FBO for configuration **E** with C–N bonding, configuration **G** with B–O bonding and configuration **H** with C–O bonding mean that the configurations have stronger intermolecular interactions. When it comes to configuration **F**, which is no WBI and FBO values, there is no interaction between the drug molecule and CBN heterofullerene. It is important to note that the interaction between N atom of favipiravir and B atom of CBN heterofullerene in the different positions has an influence on the WBI and FBO.

The scatter plots of reduced density gradient (RDG) vs. $sign(\lambda_2)\rho$ for studied configurations were presented in Fig. 9. RDG methodology allows us to survey binding properties of interactions such as attractive, repulsive, weak, or strong. It can be seen from Fig. 9 that there is attractive interaction in the range of $\rho = 0.00$ and $\rho = -0.02$ in configurations **A-F**, indicating the dominance of the effect of van der Waals forces for both attraction and repulsions between binding atoms. For configurations **G** and **H**, the RDG analyses show that there are evident deep spikes in a range of -0.02 and -0.03, which indicate stronger attractive interaction than configurations **A**−**F**.

Ultraviolet–visible (UV–vis) absorption spectra of interacting favipiravir and CBN heterofullerene are also carried out by using TD-DFT and shown in Fig. 10. The first maximum UV–vis of favipiravir and CBN heterofullerene interactions show peaks located wavelengths between 320 and 400 nm which corresponds to the near UV region and the closest UV radiation to visible light. An excitation wavelength (electron-transfer wavelength) in the visible region is preferred because ultraviolet light is harmful for living organism [49]. The second maximum peaks fluctuated wavelengths between 600 and 800 nm because of the binding points of favipiravir on CBN heterofullerene.

4. Conclusions

In this work, adsorption properties and electronic structure of the favipiravir drug on the CBN heterofullerene were carried out with DFT method. Our results show that B–O bonding in configuration **A** is stronger than that of B–N and C–O bonding, thus it is energetically more favorable. The relative energy of configuration **H**, 20.76 kcal/mol, means that it is the most reactive than that of the others and higher than the most stable configuration **A**. The adsorption energies are calculated in the range of −3.41 and −23.95 kcal/mol due to binding points of interacting atoms in favipiravir and CBN heterofullerene. The smallest value of the E_g (0.4 eV) means that charge transfer can easily occur between HOMO and LUMO energy levels, thus gives rise a change in the biological activity of favipiravir and CBN heterofullerene configuration. The molecular orbital patterns show that the HOMO is localized at the adsorbed favipiravir molecule and the LUMO is localized at the CBN heterofullerene (E, G and H configurations). From vertical ionization potential and chemical hardness, configuration **H** is the most reactive than that of the others, which means the large energy required to eject electrons from the configuration **H** and also demonstrates more resistance to charge transfer than other configurations. The WBI and FBO analyses indicate that the charge transfer occurs from the favipiravir to CBN heterofullerene. From RDG analysis, configurations **G** and **H** are stronger attractive interactions than the other configurations. The absorption peaks indicate that all configurations can absorb in range of 320–800 nm in the near and visible light region. We can conclude that the favipiravir drug on the CBN heterofullerene can be used as a delivery tool to decrease harmful effects of the favipiravir drug.

Declaration of competing interest

The authors declare that they have no known competing financial interests or personal relationships that could have appeared to influence the work reported in this paper.

Acknowledgments

The numerical calculations reported were partially performed at TUBITAK ULAKBIM, High Performance and Grid Computing Centre (TRUBA resources), Turkey.

Appendix A. Supplementary data

Supplementary data to this article can be found online at https://doi.org/10.1016/j.physe.2021.114950.

References

[1] J.-G. Park, G. Avila-Perez, A. Nogales, P. Blanco-Lobo, J.C. de la Torre, L. Martinez-Sobrido, Identification and characterization of novel compounds with broad-spectrum antiviral activity against influenza A and B viruses, J. Virol. 94 (2020), https://doi.org/10.1128/JVI.02149-19.

[2] J.D. Morrey, B.S. Taro, V. Siddharthan, H. Wang, D.F. Smee, A.J. Christensen, Y. Furuta, Efficacy of orally administered T-705 pyrazine analog on lethal West Nile virus infection in rodents, Antivir. Res. 80 (2008) 377–379, https://doi.org/10.1016/j.antiviral.2008.07.009.

[3] N. Espy, E. Nagle, B. Pfeffer, K. Garcia, A.J. Chitty, M. Wiley, M. Sanchez-Lockhart, S. Bavari, T. Warren, G. Palacios, T-705 induces lethal mutagenesis in Ebola and Marburg populations in macaques, Antivir. Res. 170 (2019), https://doi.org/10.1016/j.antiviral.2019.06.001.

[4] K. Rosenke, H. Feldmann, J.B. Westover, P.W. Hanley, C. Martellaro, F. Feldmann, G. Saturday, J. Lovaglio, D.P. Scott, Y. Furuta, T. Komeno, B.B. Gowen, D. Safronetz, Use of favipiravir to treat lassa virus infection in macaques, Emerg. Infect. Dis. 24 (2018) 1696–1699, https://doi.org/10.3201/eid2409.180233.

[5] L. Oestereich, A. Luedtke, S. Wurr, T. Rieger, C. Munoz-Fontela, S. Guenther, Successful treatment of advanced Ebola virus infection with T-705 (favipiravir) in a small animal model, Antivir. Res. 105 (2014) 17–21, https://doi.org/10.1016/j.antiviral.2014.02.014.

[6] F. Jensen, Introduction to Computational Chemistry, John Wiley & Sons, Inc., USA, 2006.

[7] S.G. Viveiros Rosa, W.C. Santos, Clinical trials on drug repositioning for COVID-19 treatment, Rev. Panam. Salud Publ./Pan Am. J. Publ. Heal. 44 (2020), https://doi.org/10.26633/RPSP.2020.40.

[8] A.S. Rad, M. Ardjmand, M.R. Esfahani, B. Khodashenas, DFT calculations towards the geometry optimization, electronic structure, infrared spectroscopy and UV-vis analyses of Favipiravir adsorption on the first-row transition metals doped fullerenes; a new strategy for COVID-19 therapy, Spectrochim. Acta, Part A Mol. Biomol. Spectrosc. 247 (2021), https://doi.org/10.1016/j.saa.2020.119082.

[9] L. Bai, X. Li, L. He, Y. Zheng, H. Lu, J. Li, L. Zhong, R. Tong, Z. Jiang, J. Shi, J. Li, Antidiabetic potential of flavonoids from traditional Chinese medicine: a review,

Am. J. Chin. Med. 47 (2019) 933–957, https://doi.org/10.1142/S0192415X19500496.
[10] P. Sharma, D.G.I. Scott, Optimizing methotrexate treatment in rheumatoid arthritis: the case for subcutaneous methotrexate prior to biologics, Drugs 75 (2015) 1953–1956, https://doi.org/10.1007/s40265-015-0486-7.
[11] M. Kurban, İ. Muz, Theoretical investigation of the adsorption behaviors of fluorouracil as an anticancer drug on pristine and B-, Al-, Ga-doped C36 nanotube, J. Mol. Liq. 309 (2020) 113209, https://doi.org/10.1016/j.molliq.2020.113209.
[12] B. Khezri, S.M.B. Mousavi, L. Krejcova, Z. Heger, Z. Sofer, M. Pumera, Ultrafast electrochemical trigger drug delivery mechanism for nanographene micromachines, Adv. Funct. Mater. 29 (2019), https://doi.org/10.1002/adfm.201806696.
[13] S. Campuzano, B. Esteban-Fernández De Ávila, P. Yáñez-Sedeño, J.M. Pingarrón, J. Wang, Nano/microvehicles for efficient delivery and (bio)sensing at the cellular level, Chem. Sci. 8 (2017) 6750–6763, https://doi.org/10.1039/c7sc02434g.
[14] A.S. Ghasemi, F. Ashrafi, S.A. Babanejad, A. Elyasi, Study of the physicochemical properties of anti-cancer drug gemcitabine on the surface of Al doped C60 and C70 fullerenes: a DFT computation, J. Struct. Chem. 60 (2019) 13–19, https://doi.org/10.1134/S0022476619010037.
[15] A.S. Ghasemi, F. Mashhadban, F. Ravari, A DFT study of penicillamine adsorption over pure and Al-doped C60 fullerene, Adsorption 24 (2018) 471–480, https://doi.org/10.1007/s10450-018-9960-3.
[16] O. V Lynchak, Y.I. Prylutskyy, V.K. Rybalchenko, O.A. Kyzyma, D. Soloviov, V. V Kostjukov, M.P. Evstigneev, U. Ritter, P. Scharff, Comparative analysis of the antineoplastic activity of C60 fullerene with 5-fluorouracil and pyrrole derivative in vivo, Nanoscale Res. Lett. 12 (2017) 8, https://doi.org/10.1186/s11671-016-1775-0.
[17] M.K. Hazrati, N.L. Hadipour, Adsorption behavior of 5-fluorouracil on pristine, B-, Si-, and Al-doped C60 fullerenes: a first-principles study, Phys. Lett. 380 (2016) 937–941, https://doi.org/10.1016/j.physleta.2016.01.020.
[18] C. Parlak, Ö. Alver, A density functional theory investigation on amantadine drug interaction with pristine and B, Al, Si, Ga, Ge doped C60 fullerenes, Chem. Phys. Lett. 678 (2017) 85–90, https://doi.org/10.1016/j.cplett.2017.04.025.
[19] E. Chigo-Anota, A. Escobedo-Morales, H. Hernández-Cocoletzi, J.G.L. y López, Nitric oxide adsorption on non-stoichiometric boron nitride fullerene: structural stability, physicochemistry and drug delivery perspectives, Phys. E Low-Dimensional Syst. Nanostructures. 74 (2015) 538–543, https://doi.org/10.1016/j.physe.2015.08.008.
[20] M. Moradi, M. Nouraliei, R. Moradi, Theoretical study on the phenylpropanolamine drug interaction with the pristine, Si and Al doped [60] fullerenes, Phys. E Low-Dimen. Syst. Nanostruct. 87 (2017) 186–191, https://doi.org/10.1016/j.physe.2016.11.027.
[21] A.S. Rad, M.H. Shahavi, M.R. Esfahani, N. Darvishinia, S. Ahmadizadeh, Are nickel- and titanium- doped fullerenes suitable adsorbents for dopamine in an aqueous solution? Detailed DFT and AIM studies, J. Mol. Liq. 322 (2021), https://doi.org/10.1016/j.molliq.2020.114942.
[22] A.S. Rad, S.M. Aghaei, Potential of metal-fullerene hybrids as strong nanocarriers for cytosine and guanine nucleobases: a detailed DFT study, Curr. Appl. Phys. 18 (2018) 133–140, https://doi.org/10.1016/j.cap.2017.11.016.
[23] A.S. Rad, S.M. Aghaei, E. Aali, M. Peyravi, M. Jahanshahi, Application of chromium-doped fullerene as a carrier for thymine and uracil nucleotides: comprehensive density functional theory calculations, Appl. Organomet. Chem. 32 (2018), e4070, https://doi.org/10.1002/aoc.4070.
[24] İ. Muz, M. Kurban, A first-principles evaluation on the interaction of 1,3,4-oxadiazole with pristine and B-, Al-, Ga-doped C60 fullerenes, J. Mol. Liq. 335 (2021) 116181, https://doi.org/10.1016/j.molliq.2021.116181.
[25] M.K. Hazrati, N.L. Hadipour, Adsorption behavior of 5-fluorouracil on pristine, B-, Si-, and Al-doped C60 fullerenes: a first-principles study, Phys. Lett. 380 (2016) 937–941, https://doi.org/10.1016/j.physleta.2016.01.020.
[26] M. Chen, R. Guan, S. Yang, Hybrids of fullerenes and 2D nanomaterials, Adv. Sci. 6 (2019), https://doi.org/10.1002/advs.201800941.
[27] S. Amiraslanzadeh, The effect of doping different heteroatoms on the interaction and adsorption abilities of fullerene, Heteroat. Chem. 27 (2016) 23–31, https://doi.org/10.1002/hc.21284.
[28] R.N. Goyal, V.K. Gupta, N. Bachheti, Fullerene-C60-modified electrode as a sensitive voltammetric sensor for detection of nandrolone—an anabolic steroid used in doping, Anal. Chim. Acta 597 (2007) 82–89, https://doi.org/10.1016/j.aca.2007.06.017.
[29] J. Shi, H. Zhang, L. Wang, L. Li, H. Wang, Z. Wang, Z. Li, C. Chen, L. Hou, C. Zhang, Z. Zhang, PEI-derivatized fullerene drug delivery using folate as a homing device targeting to tumor, Biomaterials 34 (2013) 251–261, https://doi.org/10.1016/j.biomaterials.2012.09.039.
[30] M.J. Al-Anber, A.H. Al-Mowali, A.M. Ali, Theoretical semiempirical study of the nitrone (anticancer drug) interaction with fullerene C60 (as delivery), Acta Phys. Pol. A. 126 (2014) 845–848, https://doi.org/10.12693/APhysPolA.126.845.
[31] Ş. Erkoç, Structure and electronic properties of heterofullerene C30B15N15, J. Mol. Struct. Theochem. 684 (2004) 117–120, https://doi.org/10.1016/j.theochem.2004.06.040.
[32] A. Hosseinian, A. Bekhradnia, E. Vessally, L. Edjlali, M.D. Esrafili, A theoretical study on the C 30 X 15 Y 15 (X = B, and Al; Y = N, and P) heterofullerenes, Comput. Theor. Chem. 1115 (2017) 114–118, https://doi.org/10.1016/j.comptc.2017.06.010.
[33] M. Moradi, A.A. Peyghan, Z. Bagheri, Tuning the electronic properties of C30B15N15 fullerene via encapsulation of alkali and alkali earth metals, Synth. Met. 177 (2013) 94–99, https://doi.org/10.1016/j.synthmet.2013.06.018.
[34] E. Zahedi, A. Seif, T.S. Ahmadi, Structural and electronic properties of ammonia adsorption on the C30B15N15 heterofullerene: a density functional theory study, J. Comput. Theor. Nanosci. 8 (2011) 2159–2165, https://doi.org/10.1166/jctn.2011.1938.
[35] M.K. Hazrati, Z. Bagheri, A. Bodaghi, Application of C 30 B 15 N 15 heterofullerene in the isoniazid drug delivery: DFT studies, Phys. E Low-Dimensional Syst. Nanostructures. 89 (2017) 72–76, https://doi.org/10.1016/j.physe.2017.02.009.
[36] A.D. Becke, A new mixing of hartree-fock and local density functional theories, J. Chem. Phys. 98 (1993) 1372–1377, https://doi.org/10.1063/1.464304.
[37] S. Grimme, S. Ehrlich, L. Goerigk, Effect of the damping function in dispersion corrected density functional theory, J. Comput. Chem. 32 (2011) 1456–1465, https://doi.org/10.1002/jcc.21759.
[38] M.J. Frisch, G.W. Trucks, H.B. Schlegel, G.E. Scuseria, M.A. Robb, J.R. Cheeseman, G. Scalmani, V. Barone, B. Mennucci, G.A. Petersson, H. Nakatsuji, M. Caricato, X. Li, H.P. Hratchian, A.F. Izmaylov, J. Bloino, G. Zheng, J.L. Sonnenberg, M. Hada, M. Ehara, K. Toyota, R. Fukuda, J. Hasegawa, M. Ishida, T. Nakajima, Y. Honda, O. Kitao, H. Nakai, T. Vreven, J.A. Montgomery, J.E. Peralta, F. Ogliaro, M. Bearpark, J.J. Heyd, E. Brothers, K.N. Kudin, V.N. Staroverov, R. Kobayashi, J. Normand, K. Raghavachari, A. Rendell, J.C. Burant, S.S. Iyengar, J. Tomasi, M. Cossi, N. Rega, J.M. Millam, M. Klene, J.E. Knox, J.B. Cross, V. Bakken, C. Adamo, J. Jaramillo, R. Gomperts, R.E. Stratmann, O. Yazyev, A.J. Austin, R. Cammi, C. Pomelli, J.W. Ochterski, R.L. Martin, K. Morokuma, V.G. Zakrzewski, G.A. Voth, P. Salvador, J.J. Dannenberg, S. Dapprich, A.D. Daniels, Farkas, J. B. Foresman, J. V Ortiz, J. Cioslowski, D.J. Fox, Gaussian 09, Revision E.01, Gaussian Inc., Wallingford CT, 2009.
[39] S.F. Boys, F. Bernardi, The calculation of small molecular interactions by the differences of separate total energies. Some procedures with reduced errors, Mol. Phys. 19 (1970) 553–566, https://doi.org/10.1080/00268977000101561.
[40] B.M. Wong, T.H. Hsieh, Optoelectronic and excitonic properties of oligoacenes: substantial improvements from range-separated time-dependent density functional theory, J. Chem. Theor. Comput. 6 (2010) 3704–3712, https://doi.org/10.1021/ct100529s.
[41] M.E. Foster, B.M. Wong, Nonempirically tuned range-separated DFT accurately predicts both fundamental and excitation gaps in DNA and RNA nucleobases, J. Chem. Theor. Comput. 8 (2012) 2682–2687, https://doi.org/10.1021/ct300420f.
[42] R.G. Pearson, The principle of maximum hardness, Acc. Chem. Res. 26 (1993) 250–255, https://doi.org/10.1021/ar00029a004.
[43] T. Lu, F. Chen, Multiwfn: a multifunctional wavefunction analyzer, J. Comput. Chem. 33 (2012) 580–592, https://doi.org/10.1002/jcc.22885.
[44] M. Zaboli, H. Raissi, The analysis of electronic structures, adsorption properties, NBO, QTAIM and NMR parameters of the adsorbed hydrogen sulfide on various sites of the outer surface of aluminum phosphide nanotube: a DFT study, Struct. Chem. 26 (2015) 1059–1075, https://doi.org/10.1007/s11224-015-0563-2.
[45] N.M. O'Boyle, A.L. Tenderholt, K.M. Langner, cclib, A library for package-independent computational chemistry algorithms, J. Comput. Chem. 29 (2008) 839–845, https://doi.org/10.1002/jcc.20823.
[46] M.A. Salem, K.P. Katin, S. Kaya, A.I. Kochaev, M.M. Maslov, Interaction of dopants and functional groups adsorbed on the carbon fullerenes: computational study, Phys. E Low-Dimensional Syst. Nanostructures. 124 (2020), https://doi.org/10.1016/j.physe.2020.114319.
[47] N.R. Abdullah, H.O. Rashid, M.T. Kareem, C.-S. Tang, A. Manolescu, V. Gudmundsson, Effects of bonded and non-bonded B/N codoping of graphene on its stability, interaction energy, electronic structure, and power factor, Phys. Lett. 384 (2020), https://doi.org/10.1016/j.physleta.2020.126350.
[48] N.R. Abdullah, H.O. Rashid, C.-S. Tang, A. Manolescu, V. Gudmundsson, Modeling electronic, mechanical, optical and thermal properties of graphene-like BC6N materials: role of prominent BN-bonds, Phys. Lett. 384 (2020), https://doi.org/10.1016/j.physleta.2020.126807.
[49] S.C. Burdette, S.J. Lippard, ICCC34 - golden edition of coordination chemistry reviews. Coordination chemistry for the neurosciences, Coord. Chem. Rev. 216 (2001) 333–361, https://doi.org/10.1016/S0010-8545(01)00308-3.